Engineering

Electrical Engineering fields

Okayama University *Year* 1989

A control strategy of three-phase PWM inverter with fluctuating input voltage

Shigeyuki Funabiki
Okayama University

A Control Strategy of Three-Phase PWM Inverter with Fluctuating Input Voltage

Shigeyuki FUNABIKI
Dept. of Electrical and Electronic Engineering
Okayama University, Okayama 700, Japan

Abstract A digital control strategy of the three-phase PWM inverter is proposed for the sinusoidal output with fluctuating input voltage. The pulse width is computed by sampling and predicting the fluctuating input voltage every time the pulse generates. The three predictive methods are proposed. The errors and the waveform distortion of the output voltage are analyzed and discussed with the proposed predictive methods. The validity of the proposed control method is experimentally verified by using the microprocessor-based control system. The preestimate is proved to be the most available method in the three predictive methods.

INTRODUCTION

A microprocessor-based control system is widely used for controlling power converters. Y. H. Kim et al. proposed an algebraic method of pulse width modulation in a single-phase inverter suitable for a microprocessor-based control system [1]. The authors also proposed the computative method of pulse width for the three-phase sin-wave PWM inverter [2].

A dc voltage supply for the PWM inverter is usually obtained by rectifying an ac voltage. Then, the rectified voltage has the fluctuating components due to the behavior of the rectifier, especially the component with a twice frequency of the ac supply. Therefore, the control method of the sin-wave PWM inverter with fluctuating input voltage is required to be developed for industrial applications. J. Lee et al. proposed the control method of the PWM inverter with fluctuating input voltage based on the triangulation method [3]. In this method, the AD and DA conversion are required at large number of times as compared with the number of pulse. The flux-controlled real time PWM was applied to the PWM inverter with fluctuating input voltage [4].

In this paper, a digital control strategy is proposed for a three-phase sin-wave PWM inverter with fluctuating input voltage. The pulse width is computed by sampling and predicting the fluctuating input voltage every time the pulse generates. The three predictive methods, the hold approximation, the straight line approximation and the preestimate, are proposed. The errors and the waveform distortion of the output voltage are analyzed and discussed with the proposed predictive methods. The validity of the proposed control method is experimentally verified by using the microprocessor-based control system.

DECISION OF PULSE WIDTH OF PWM INVERTER

PWM Inverter and Output Voltage Command

Fig. 1 shows a simplified model of a three-phase PWM inverter with fluctuating input voltage. The PWM inverter comprises a dc supply, six switches and a three-phase load. The dc voltage is usually gained by rectifying the ac voltage. Then, the rectified voltage has the fluctuating components due to the behavior of the rectifier.

Superimposing the 3rd harmonic to increase an output voltage of the PWM inverter, the output voltage command of phase-A $v_{AO}^*(t)$ is obtained by

$$v_{AO}^*(t) = V^* \sin(\omega_i t) + V_3 \sin(3\omega_i t) \quad (1)$$

where

V^* amplitude of output voltage command

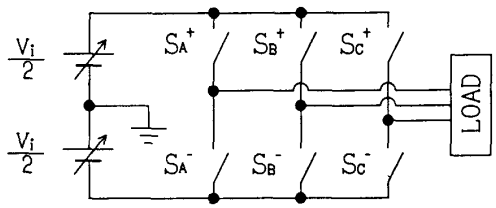

Fig. 1 Simplified model of three-phase PWM inverter

V_3 amplitude of the 3rd harmonic ($V_3=V^*/6$)
ω_i angular output frequency of PWM inverter ($=2\pi f_i$, f_i is the inverter output frequency)

Decision of Pulse Width

An output voltage command in phase-A, an input voltage and a switching behavior of the switches in the corresponding inverter leg are shown in Fig. 2. In this figure, n_p is the number of dividing an half cycle of PWM inverter performance, $v_{AO}^*(t)$ is the output voltage command in phase-A, $v_{AO}^*(k)$ and $v_{AO}^*(k+1)$ are the values of the output voltage command in phase-A at the point of k and (k+1). Further, $v_i(t)$ is the input voltage of the PWM inverter, and $v_i(k-3)$, $v_i(k-2)$, $v_i(k-1)$ and $v_i(k)$ are the sampled values at the point of (k-3), (k-2), (k-1) and k. The switching pulse "1" or "0" indicates that the switch in the upper leg or in the lower leg is conducting. The pulse width is numerically computed by using the areas S_1 and S_2 [2].

The average value of the output voltage command $V_{AO}^*(k)$ in the k-th period is calculated by

$$V_{AO}^*(k) = \int_{(k-1)\Delta t}^{k\Delta t} v_{AO}^*(t)dt/\Delta t \quad (2)$$

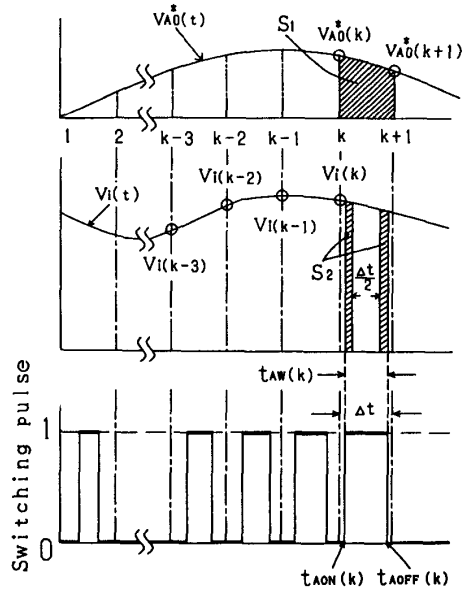

Fig. 2 Output voltage command and switching behavior

89CH2792-0/89/0000-1170$01.00 © 1989 IEEE

where
Δt $=1/(2n_p f_i)$ time of one period

Integrating the output voltage of phase-A in the k-th period, the next equation is derived.

$$\int_{(k-1)\Delta t}^{k\Delta t} v_{AO}(t)dt = \int_0^{t_{AW}(k)} \{V_i(k)/2\}dt + \int_0^{\Delta t - t_{AW}(k)} \{-V_i(k)/2\}dt$$

$$= V_i(k)\{t_{AW}(k) - \Delta t/2\} \quad (3)$$

where
$V_i(k)$ average value of $v_i(t)$ in the k-th period
$t_{AW}(k)$ on-time of the switch in the upper leg in phase-A

The next equation is gained by making (3) equal to $V_{AO}^*(k)\Delta t$.

$$V_i(k)\{t_{AW}(k) - \Delta t/2\} = V_{AO}^*(k)\Delta t \quad (4)$$

Therefore, $t_{AW}(k)$ in Fig. 2 is decided by equaling the area S_1 to the area S_2. Then, we obtain

$$t_{AW}(k) = \frac{V_{AO}^*(k)}{V_i(k)} - \frac{1}{2}\Delta t \quad (5)$$

Then, a switch-on and switch-off time of the switch S_A^+ are computed as follows;

$$t_{AON}(k) = \frac{2k-1}{2}\Delta t - \frac{t_{AW}(k)}{2} \quad (6)$$

$$t_{AOFF}(k) = \frac{2k-1}{2}\Delta t + \frac{t_{AW}(k)}{2} \quad (7)$$

On the other hand, the switch S_A^- behaves by contrast to the switch S_A^+. The on-time in other legs of the PWM inverter are also calculated in the same procedure.

Prediction of Fluctuating Input Voltage

In the proposed control strategy, the average value of fluctuating input voltage in each period when the on-time of the switch may be calculated must be required. However, the average value of the input voltage is unknown at the time of calculating the on-time of the switch. Then, it is necessary to predict the average value of the input voltage.

The average value of the input voltage $V_i(k)$ in the k-th period is predicted in the next methods.

(a) hold approximation

$V_i(k)$ is predicted by

$$V_i(k) = v_i(k) \quad (8)$$

(b) straight line approximation

$V_i(k)$ is predicted by using the value of $v_i(k-1)$ and $v_i(k)$.

$$V_i(k) = \{3v_i(k) - v_i(k-1)\}/2 \quad (9)$$

(c) preestimate

(c-1) preestimate I

$v_i(k)$ and $v_i(k+1)$ are predicted by using $v_i(k-1)$, $v_i(k-2)$ and $v_i(k-3)$.

$$v_i(k) = v_i(k-1) + \{v_i(k-1) - v_i(k-2)\}$$
$$v_i(k+1) = v_i(k-1) + \{v_i(k-1) - v_i(k-3)\} \quad (10)$$

Then, $V_i(k)$ is calculated by

$$V_i(k) = \frac{v_i(k)+v_i(k+1)}{2}$$

$$= \frac{4v_i(k-1)-v_i(k-2)-v_i(k-3)}{2} \quad (11)$$

(c-2) preestimate II

The fluctuating input voltage is approximated by the next quadratic equation.

$$v_i(t) = k_1t^2 + k_2t + k_3 \quad (12)$$

Setting the (k-3) point to the reference time, the coefficients k_1, k_2 and k_3 are obtained by

$$k_1 = \frac{v_i(k-1)-2v_i(k-2)+v_i(k-3)}{2} \quad (13)$$

$$k_2 = \frac{-v_i(k-1)+4v_i(k-2)-3v_i(k-3)}{2} \quad (14)$$

$$k_3 = v_i(k-3) \quad (15)$$

Then, we get

$$V_i(k) = \frac{v_i(k)+v_i(k+1)}{2}$$

$$= \frac{9v_i(k-1)-11v_i(k-2)+4v_i(k-3)}{2} \quad (16)$$

ANALYSIS OF OUTPUT VOLTAGE

In this chapter, the validity of the proposed control strategy is discussed from the waveform analysis of the output voltage. The Fourier series of the output voltage in phase-A is expressed by

$$v_{AO}(x) = \frac{a_0}{2} + \sum_{n=1}^{\infty}\{a_n\sin(nx) + b_n\sin(nx)\} \quad (17)$$

where $x=\omega_i t$.

From Fig. 1, the terminal voltage in phase-A is expressed by

$$v_{AO}(x) = \begin{cases} V_i(k)/2 & x_{AON}(k) \le x < x_{AOFF}(k) \\ -V_i(k)/2 & (k-1)\Delta x \le x < x_{AON}(k) \\ & x_{AOFF}(k) \le x < k\Delta x \end{cases} \quad (18)$$

where $\Delta x=\omega_i \Delta t$, $x_{AON}(k)=\omega_i t_{AON}(k)$ and $x_{AOFF}(k)=\omega_i t_{AOFF}(k)$.

The fundamental component of the output voltage in phase-A is derived as follows;

$$a_1 = \frac{1}{\pi}\int_0^{2\pi} v_{AO}(x)\sin(x)dx$$

$$= \frac{1}{\pi}\sum_{k=1}^{n_p} V_i(k)\{2\sin\left(\frac{x_{AW}(k)}{2}\right) - \sin\left(\frac{\Delta x}{2}\right)\}\sin\left(\frac{2k-1}{2}\Delta x\right) \quad (19)$$

where $x_{AW}(k)=\omega_i t_{AW}(k)$.

From the Taylor series, and $\cos(\beta)=1$ and $\sin(\beta)=\beta$ when β is small, (19) is rewritten by

$$a_1 = \frac{1}{\pi}\sum_{k=1}^{n_p}\{V^*\Delta x \sin^2\left(\frac{2k-1}{2}\Delta x\right) + \frac{V^*}{6}\Delta x \sin\left(\frac{3(2k-1)}{2}\Delta x\right)\sin\left(\frac{2k-1}{2}\Delta x\right)\}$$

$$= \frac{1}{\pi}\int_0^{2\pi} V^*\{\sin(x) + \frac{1}{6}\sin(3x)\}\sin(x)dx$$

$$= V^* \qquad (20)$$

In the same manner, b_1 is derived as

$$b_1 = \frac{1}{\pi}\int_0^{2\pi} v_{AO}(x)\cos(x)dx$$

$$= \frac{1}{\pi}\sum_{k=1}^{n_p} V_i(k)\{2\sin\left(\frac{x_{AW}(k)}{2}\right) - \sin\left(\frac{\Delta x}{2}\right)\}\cos\left(\frac{2k-1}{2}\Delta x\right)$$

$$= \frac{1}{\pi}\sum_{k=1}^{n_p}\{V^*\Delta x \sin\left(\frac{2k-1}{2}\Delta x\right) + \frac{V^*}{6}\Delta x \sin\left(\frac{3(2k-1)}{2}\Delta x\right)\}$$

$$\times\cos\left(\frac{2k-1}{2}\Delta x\right)$$

$$= \frac{1}{\pi}\int_0^{2\pi} V^*\{\sin(x) + \frac{1}{6}\sin(3x)\}\cos(x)dx$$

$$= 0 \qquad (21)$$

The line-to-line output voltage $v_{AB}(t)$ is derived by the output terminal voltage $v_{AO}(t)$ and $v_{BO}(t)$. Therefore, the aboved results show that the PWM inverter based on the proposed control technique produces the output voltage in accordance with the output voltage command.

CONTROL SYSTEM OF PWM INVERTER AND PREDICTION METHOD

The control system of the proposed PWM inverter is shown in Fig. 3. The control system detects the input voltage and calculates the pulse width, and then activates the switching devices through the drive circuit. The processing of predicting the input voltage, calculating the pulse width and generating the pulse is executed in the interrupt routine controlled by the programmable interrupt controller (8259). The main routine executes the initialization of the control system and the calculation of V_{AO}^*, V_{BO}^* and V_{CO}^*.

Fig. 4 shows the flow chart of the interrupt routine at the k-th period. The flow charts are shown in Fig. 4(a) for the prediction (a) and (b), and shown in Fig. 4(b) for the prediction (c), respectively. In the prediction (a) and (b), the input voltage is sampled and converted, and then $V_i(k)$ is predicted and the pulse width in this period is calculated. After that, the pulse is generated.

On the other hand, in the prediction (c), the input voltage is sampled in the first place, and then the pulse is generated. After that, the sampled data is converted, and then $V_i(k+1)$ is predicted and the pulse width in the next period is calculated. Namely, the pulse width in the k-th period has been calculated in the preceding period.

The time for predicting the input voltage and calculating the pulse width is much longer than that for sampling and holding the data. For example, the former is about 300 μs and the latter is about 20 μs in the control system shown in Fig. 3 in which the cpu is

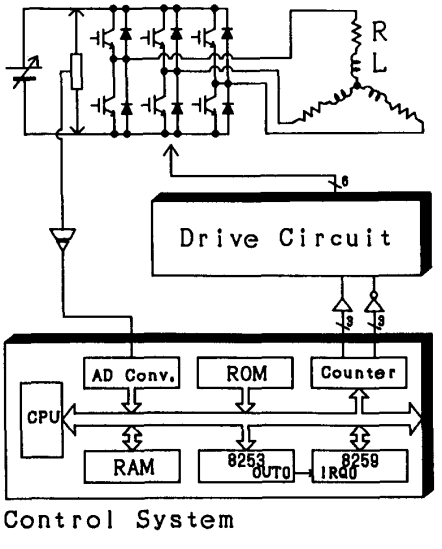

Fig. 3 Control system of proposed PWM inverter

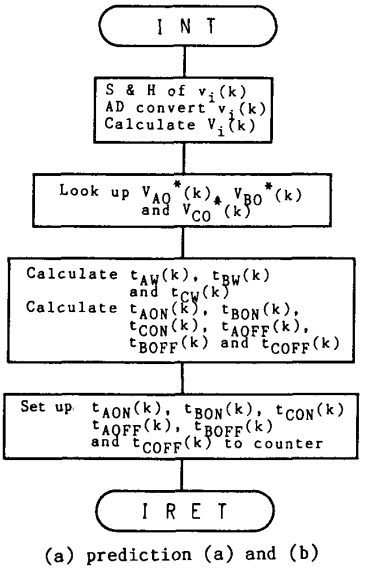

(a) prediction (a) and (b)

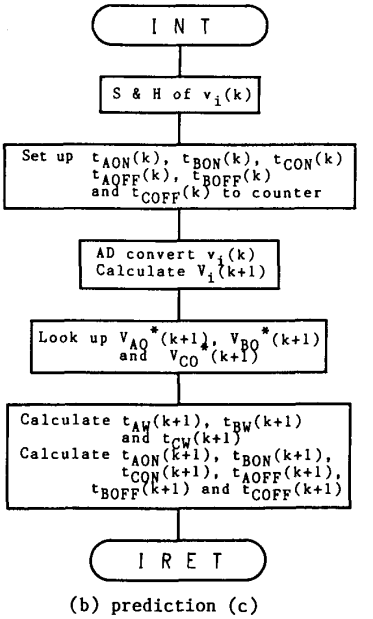

(b) prediction (c)

Fig. 4 Flow chart of interrupt

8086 at 5 MHz. Therefore, the maximum on-time of the switch in the prediction (c) is much longer than that in the prediction (a) and (b). Consequently, the control method using the prediction (c) is superior to that using the prediction (a) and (b).

ANALYSIS OF PWM INVERTER OUTPUT VOLTAGE

Error of Output Voltage

In this chapter, the control characteristics of the output voltage are discussed by analysis. In the proposed control technique, some assumptions are introduced. Therefore, the error between the output voltage command and the produced voltage occur. Then, in the analysis, the fluctuating input voltage is assumed by

$$v_i(t) = V_{dc}\{1 + \delta\sin(\frac{2\pi f_i}{\alpha}t+\theta)\} \quad (22)$$

where

V_{dc} dc component of fluctuating input voltage
δ $= V_{ac}/V_{dc}$
V_{ac} ac component of fluctuating input voltage
α $= f_i/f_{ac}$
f_{ac} frequency of ac component
θ phase angle, 0 to 2π

Further, the ratio of the output voltage command to the dc component of fluctuating input voltage is introduced as $\kappa = 2V^*/V_{dc}$. The error of output voltage is expressed by

$$\varepsilon_V = \left|\frac{V_0-\sqrt{3}V^*}{\sqrt{3}V^*}\right| \times 100 \quad (23)$$

where

V_0 the fundamental component of the line-to-line output voltage

Table 1 and 2 show the maximum error among ones at all phase angles for n_p and for δ, respectively. In the tables, the values in (d) indicate the maximum errors without the modification of the pulse width according to the fluctuation of the input voltage.

It is seen from Table 1 that the error in the output voltage can be considerably improved by the proposed control technique. As n_p becomes larger, the error becomes smaller. Although the error in the method (c) is large in the small value of n_p, it becomes as small as that in the other predictive methods as n_p becomes larger. Namely, the error in the method (c-2) becomes same as that in the method (b) at n_p above 33. Further, the error in the method (c-1) is smaller than that in the method (a) at n_p above 33. It is found from Table 2 that the error becomes larger as the fluctuating component becomes larger.

Consequently, the proposed methods are useful from a viewpoint of the error of the output voltage. Then, the PWM technique with the large n_p using the method (c) is most available.

Distortion of Output Voltage

In this section, the waveform of the output voltage is discussed from a view of the total harmonic distortion (THD). THD is expressed by

$$THD = \sqrt{\sum_{n=2}^{\infty}\left(\frac{C_n}{nC_{10}}\right)^2} \quad (24)$$

where

C_{10} fundamental components of output voltage
C_n n-th harmonic of output voltage

Table 3 and 4 show the THD for n_p and for δ, respectively. Although the THD in the method (c) is larger than those in the methods (a) and (b) in the small value of n_p, it becomes as small as that in the other predictive methods. That is because the lower-order harmonics, especially the 3rd harmonic, generate larger than those in the method (a) and (b) in the small value of n_p with the method (c). However, the 3rd harmonic is rapidly reduced as n_p becomes larger. The THD becomes larger with the increase of δ.

Therefore, the amplitude of the fluctuating component should be properly limited from a viewpoint of the harmonics in the output voltage waveform.

EXPERIMENT

Experimental System

The experiment is carried out using the rectifier shown in Fig. 5 as the dc supply and the control system shown in Fig. 3. The dc voltage is gained by rectifying the ac voltage using the diode bridge. The switching devices used in the PWM inverter are IGBTs.

Table 1 Maximum error for n_p

n_p	(a)	(b)	(c-1)	(c-2)	(d)
9	4.3	2.3	13.6	9.4	10.8
15	2.4	0.9	4.9	1.7	10.3
21	1.7	0.4	2.5	0.7	10.2
27	1.3	0.3	1.5	0.4	10.1
33	1.0	0.2	1.0	0.2	10.1
39	0.9	0.1	0.7	0.1	10.0
60	0.6	0.1	0.3	0.1	10.0
90	0.4	0.0	0.1	0.0	10.0

α=0.5, δ=0.2, κ=0.6

Table 2 Maximum error for δ

δ	(a)	(b)	(c-1)	(c-2)	(d)
0	0.2	0.2	0.2	0.2	0.2
0.05	0.5	0.3	0.7	0.3	2.7
0.1	0.9	0.3	1.1	0.5	5.2
0.15	1.3	0.4	1.7	0.6	7.7
0.2	1.7	0.4	2.5	0.7	10.2
0.25	2.0	0.5	3.4	0.9	12.7
0.3	2.4	0.6	4.4	1.0	15.1

n_p=21, α=0.5, κ=0.6

Table 3 THD for n_p

n_p	(a)	(b)	(c-1)	(c-2)	(d)
9	3.48	3.36	4.72	4.03	4.91
15	2.06	1.96	2.35	2.00	4.12
21	1.46	1.39	1.54	1.39	3.89
27	1.14	1.07	1.15	1.07	3.80
33	0.93	0.88	0.92	0.88	3.75
39	0.78	0.74	0.77	0.74	3.72
60	0.51	0.48	0.49	0.48	3.68
90	0.34	0.32	0.32	0.32	3.66

α=0.5, δ=0.2, κ=0.6, θ=0.0(rad/s)

Table 4 THD for δ

δ	(a)	(b)	(c-1)	(c-2)	(d)
0	1.30	1.30	1.30	1.30	1.30
0.05	1.33	1.32	1.34	1.32	1.57
0.1	1.37	1.34	1.39	1.34	2.19
0.15	1.41	1.37	1.46	1.37	2.99
0.2	1.46	1.39	1.54	1.39	3.89
0.25	1.52	1.41	1.64	1.41	4.87
0.3	1.58	1.43	1.74	1.44	5.90

n_p=21, α=0.5, κ=0.6, θ=0.0(rad/s)

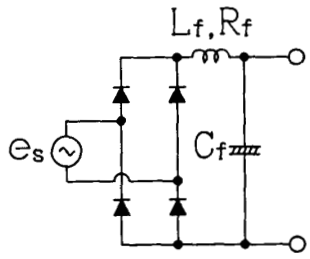

Fig. 5 Rectifier

A CPU used in the control system is a 16-bit microprocessor 8086. The input voltage is fed back to the control system through the isolation amplifier. The pulse width is computed by the control system and fed to the drive circuit through the 16-bit counter.

Experimental Results

Figs. 6 and 8 shows the waveforms of the capacitor voltage, the output voltage and the load current with the experimental condition in Tables 5 and 6, respectively. The correponding harmonic analysis of the output voltage waveform is shown in Figs. 7 and 9. As shown in Figs. 6(a) and 8(a), the capacitor voltage is found to be a dc voltage with fluctuating components due to the behaviors of the rectifier and the PWM inverter. The influence of fluctuating input voltage appears in the amplitude of the output voltage waveform in Figs. 6(b) and 8(b). However, the lower-

Table 5 Experiment condition I

AC supply		100 V, 60 Hz
inductance of LC filter	L_f	3.5 mH
resistance of LC filter	R_f	0.08 Ω
capacitance of LC filter	C_f	194 μF
inverter frequency	f_i	40 Hz
the number of pulse	$2q_p$	15
output voltage command	V^*_p	19.1 V
prediction		(a)
inductance of load	L	9 mH
resistance of load	R	1.4 Ω

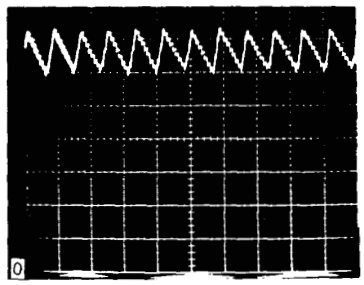

(a) capacitor voltage
20 V/div 10 ms/div

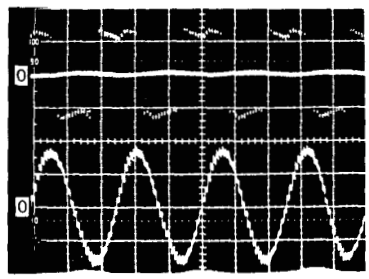

(b) output voltage and load current
upper : output voltage 108 V/div
lower : load current 4 A/div
horiszontal : 10 ms/div

Fig. 6 Waveforms on condition of Table 5

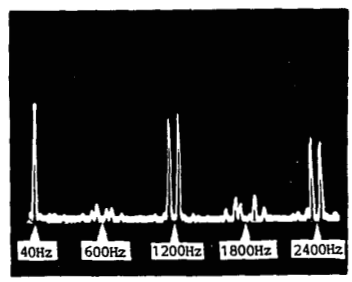

Fig. 7 Harmonic analysis of output voltage waveform on condition of Table 5

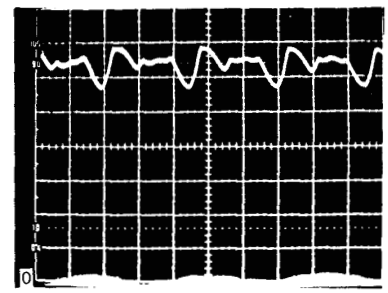

(a) capacitor voltage
20 V/div 10 ms/div

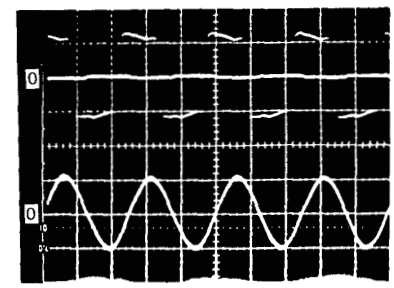

(b) output voltage and load current
upper : output voltage 108 V/div
lower : load current 12 A/div
horiszontal : 10 ms/div

Fig. 8 Waveforms on condition of Table 6

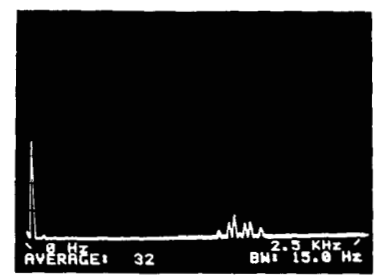

Fig. 9 Harmonic analysis of output voltage waveform on condition of Table 6

Table 6 Experiment condition II

AC supply		100 V,	60 Hz
inductance of LC filter	L_f	3.5	mH
resistance of LC filter	R_f	0.08	Ω
capacitance of LC filter	C_f	1000	μF
inverter frequency	f_i	40	Hz
the number of pulse	$2n_p$	39	
output voltage command	V^*_p	38.3	V
prediction		(c-1)	
inductance of load	L	9	mH
resistance of load	R	1.4	Ω

order harmonics due to the fluctuation in the input voltage waveform do not appear in the output waveform of the PWM inverter shown in Figs. 7 and 9.

The measured amplitudes of line-to-line output voltage are 29.8 V and 59.8 V in the condition of Table 5 and Table 6, respectively. Then, the errors are 10.0 % and 9.8 % in the condition of Table 5 and Table 6, respectively. The error in the experiment is larger than that in the analysis because of the loss in the IGBTs and diodes, and the waveform of the input voltage. The maximum line-to-line output voltage in the condition of Table 5 is about 34 V in amplitude. On the other hand, that in the condition of Table 6 is 77.4 V in amplitude. Then, it is clarified that the control method with the prediction (c) is superior to that with the prediction (a) and (b).

CONCLUSIONS

The new method of pulse width decision is proposed for a three-phase sin-wave PWM inverter. The validity of the proposed PWM technique is theoretically made clear with respect to the error of the output voltage and the THD of the output voltage waveform. It is found that a sufficient accuracy is obtained from the analytical results of the error of the output voltage vs. the number of pulses and the fluctuation of the input voltage. Furthermore, it is clarified from the algorithm of the calculating the pulse width that the predictive method (c) is most available one. Finally, the proposed PWM technique is proved effective by the experiment using the microprocessor-based control system.

REFERENCES

(1) Y. H. Kim and M. Ehsani : " An Algebraic Algorithm for Microcomputer-Based (Direct) Inverter Pulse-width Modulation " IEEE Trans. Ind. Appl., Vol.IA-23, No.4, pp.654-660 1987

(2) S. Funabiki and Y. Sawada : " A Computative Decision of Pulse Width in Three-Phase PWM Inverter " IEEE IAS 1988 Annual Meeting Record, Part I, pp.694-699 1988

(3) Jia-You Lee and York-Yih Sun : " Adaptive Harmonic Control in PWM Inverters with Fluctuating Input Voltage " IEEE Trans. Ind. Elect., Vol.IE-33, No.1, pp.92-98 1986

(4) T. Takeshita and N. Matsui : " One -chip Microcomputer-based Flux-controlled Real Time PWM ", Trans. on IEE of Japan, Vol.105-B, No.6, pp.531-538 1985